

# Nonlinear Competition Between Small and Large Hexagonal Patterns

Mary Silber

*Department of Engineering Sciences and Applied Mathematics, Northwestern University, Evanston, IL 60208 USA*

Michael R.E. Proctor

*Department of Applied Mathematics and Theoretical Physics, University of Cambridge, Cambridge CB3 9EW UK*

(Submitted: 11 September 1997)

Recent experiments by Kudrolli, Pier and Gollub [1] on surface waves, parametrically excited by two-frequency forcing, show a transition from a small hexagonal standing wave pattern to a large triangular superlattice pattern. We show that generically the small hexagonal and the large triangular wave patterns bifurcate *simultaneously* from the flat surface state as the forcing amplitude is increased, and that the experimentally-observed transition can be described by considering a low-dimensional degenerate bifurcation problem. In particular, the transition from the small hexagonal pattern to the triangular superlattice pattern can be favored over the ubiquitous hexagons-to-rolls transition.

PACS numbers: 47.20.Ky, 47.54.+r

The phenomenon of Faraday waves, which arise when vertical vibration destabilizes the free surface of a fluid layer has been widely investigated for many years [2]. In recent times there has been much interest in the nonlinear patterns formed by these waves. In an extended layer the relative stability of different patterns is determined by nonlinear effects, and well-established symmetry arguments can be deployed to explain many results. The Faraday experiment, which exhibits a wide variety of patterns, has proved a valuable testbed for the theoretical predictions.

In this letter we address recent experimental investigations of Kudrolli, Pier and Gollub [1] which employ two-frequency vertical acceleration. While for single frequency vibration the most unstable solutions are subharmonic with respect to the vibration frequency, with two frequencies harmonic response can occur [3,4]. In particular, for the patterns described here the acceleration has the form  $f(t) = a(\cos(\chi) \cos(6\omega t) + \sin(\chi) \cos(7\omega t + \phi))$ , where  $a$ ,  $\chi$  and  $\phi$  are parameters that can be varied. In the experiments, parameters are chosen to produce a standing wave pattern in the form of ‘hexagons’ at the onset of the instability. Then, as the acceleration is increased, there is a transition to a new pattern, shown in Figure 1, which Kudrolli *et al.* [1] call a superlattice pattern due to its apparent structure on two disparate length-scales. This new state has only triangular symmetry, rather than full hexagonal symmetry, and is (approximately) periodic on a hexagonal lattice, but on a larger scale than the initial hexagons. Examination of the spatial Fourier transform of the two different states

reveals that the new state is formed from the nonlinear interaction of twelve prominent Fourier modes whose wavenumbers have the same modulus  $k_c$  and lie on a hexagonal lattice with fundamental wavenumber  $k_c/\sqrt{7}$ ; Figure 2 shows the geometry.

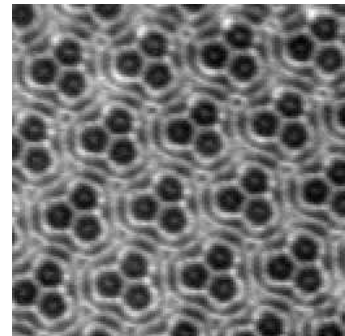


FIG. 1. The experimental superlattice-I pattern [1] (courtesy of A. Kudrolli, B. Pier and J.P.Gollub). Note the underlying hexagonal lattice and the local triangular symmetry.

Complex patterns of the type shown in Figure 1 might be expected at large amplitude where modes on different scales are excited. In this letter we show that, remarkably, this new pattern can be closely approximated by superimposing Fourier modes with only a *single* horizontal wavenumber. Furthermore, we show that the pattern in Figure 1 can arise *directly* from the flat state via a transcritical bifurcation. In this respect the pattern has much in common with hexagons. The existence of transcritical superlattice solution branches thus impinges on conventional arguments for the appearance of hexagons in systems lacking up-down symmetry [7]. In particular, we show that the observed transition from hexagons to the superlattice pattern can be favored over the familiar transition from hexagons to rolls that occurs, for example, in non-Boussinesq Rayleigh-Bénard convection [5]. (See [6] for another case where the hexagon-to-rolls transition is suppressed.) The observed pattern is distinguished from somewhat similar patterns that are characterized by two or more different horizontal scales, as in the superlattice-II state in [1], and for  $1:\sqrt{2}$  resonance on the square lattice [8].

The observed patterns are put into a theoretical framework by restricting the analysis to solutions that tile the plane in a hexagonal fashion. This choice is motivated

by the experiments, which lack up-down reflection symmetry. In the Faraday problem the reflection symmetry is associated with the subharmonic instability of the free surface. It is absent in the present setting in which the two-frequency forcing leads to harmonic standing waves [3].

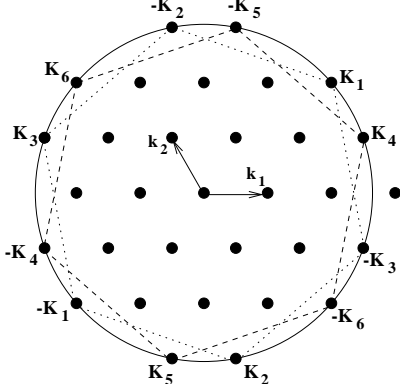


FIG. 2. Intersection of the critical circle  $|\mathbf{k}| = k_c$  with the  $\mathbf{k}$ -space hexagonal lattice generated by  $\mathbf{k}_1, \mathbf{k}_2$ . In this example  $\alpha = 3, \beta = 2$  in (2), *i.e.*,  $|\mathbf{k}_1| = |\mathbf{k}_2| = k_c/\sqrt{7}$  with  $\mathbf{K}_1 = 3\mathbf{k}_1 + 2\mathbf{k}_2$ , *etc.*. The critical wave vectors  $\pm\mathbf{K}_1, \dots, \pm\mathbf{K}_3$  lie at the vertices of a hexagon (indicated by a dotted line), as do the wave vectors  $\pm\mathbf{K}_4, \dots, \pm\mathbf{K}_6$ .

The time-periodic forcing in the Faraday problem leads us to formulate the problem in terms of a stroboscopic map. Since we seek spatially doubly-periodic solutions, we express all fields in terms of double Fourier series; for example, the height of the free surface, at time  $t = mT$ , is

$$\zeta_m(\mathbf{x}) = \text{Re} \left( \sum_{\mathbf{n} \in \mathbf{Z}^2} w_{\mathbf{n}}(mT) e^{i(n_1 \mathbf{k}_1 + n_2 \mathbf{k}_2) \cdot \mathbf{x}} \right), \quad (1)$$

where  $m$  is an integer and  $T$  is the period of the forcing. We obtain patterns periodic on a hexagonal lattice when the primitive vectors  $\mathbf{k}_1, \mathbf{k}_2$  satisfy  $|\mathbf{k}_1| = |\mathbf{k}_2| = k$  and  $\mathbf{k}_1 \cdot \mathbf{k}_2 = -\frac{1}{2}k^2$ . A standard *ansatz* in pattern selection problems is to set  $k = k_c$ , where  $k_c$  is the critical wavenumber of the instability. However, here we want to investigate competition between small and large hexagonal patterns, which we do by following the approach in [6]. Specifically, we choose  $k$  so that there are twelve wave vectors  $\mathbf{K}_n = n_1 \mathbf{k}_1 + n_2 \mathbf{k}_2$  in (1) that satisfy  $|\mathbf{K}_n| = k_c$ , *i.e.*, so that there exists a co-prime integer pair  $\mathbf{n} = (\alpha, \beta)$ ,  $\alpha > \beta > 0$ , such that

$$|\alpha \mathbf{k}_1 + \beta \mathbf{k}_2| = k \sqrt{\alpha^2 + \beta^2 - \alpha\beta} = k_c. \quad (2)$$

An example associated with  $\alpha = 3, \beta = 2, k_c/k = \sqrt{7}$  is presented in Figure 2. Note that the lattice points that lie on the critical circle are placed at the vertices of two hexagons rotated by an angle  $\theta$  relative to each other, where  $\cos(\theta) = \frac{\alpha^2 + 2\alpha\beta - 2\beta^2}{2(\alpha^2 - \alpha\beta + \beta^2)}$  [6]. If only those modes associated with one of the hexagons are excited, then

the periodicity of the pattern is dictated by  $k_c$  and one recovers the standard six-dimensional hexagonal lattice bifurcation problem. However, if all twelve modes on the critical circle are excited, then the period of the pattern is greater by a factor of  $k_c/k$  [9]; see Figure 3.

In formulating the bifurcation problem, we assume that the trivial state of the system, which corresponds to the fluid surface being flat, loses stability to harmonic waves of wavenumber  $k_c$  as a bifurcation parameter  $\lambda$  is increased through zero. Thus the Faraday instability sets in when a Floquet multiplier  $\mu$  crosses the unit circle at  $\mu = 1$ . In our formulation there are twelve (real) Fourier modes in (1) that are neutrally stable at  $\lambda = 0$ ; all others are damped. In this case the stroboscopic map can be reduced, near the onset of the instability, to a twelve-dimensional center manifold spanned by the critical Fourier modes. Let  $z_j(m)$ ,  $j = 1, \dots, 6$ , be the complex amplitude, at  $t = mT$ , of the Fourier mode  $e^{i\mathbf{K}_j \cdot \mathbf{x}}$ , with  $\bar{z}_j$  being the amplitude of  $e^{-i\mathbf{K}_j \cdot \mathbf{x}}$ . Here the  $\mathbf{K}_j$  are labeled as in Figure 2.

We assume that the bifurcation parameter  $\lambda$  has been scaled so that the linearization of the stroboscopic map

$$\mathbf{z}(m+1) = \mathbf{f}(\mathbf{z}(m)) \quad (3)$$

is  $\mathbf{z}(m+1) = (1 + \lambda)\mathbf{z}(m)$ ,  $\mathbf{z} = (z_1, z_2, z_3, z_4, z_5, z_6)$ . The possible nonlinear terms in the map are restricted by the symmetry of the problem; they are given in [6]. The values of  $\alpha$  and  $\beta$  in (2) enter through high-order resonant interaction terms in the map. For example, the first component of the map  $\mathbf{f}$  has the general form

$$f_1 = h_1(\mathbf{u}, \mathbf{q})z_1 + h_2(\mathbf{u}, \mathbf{q})\bar{z}_2\bar{z}_3 + e_1\bar{z}_1^{\alpha-\beta-1}z_3^\beta z_4^\beta \bar{z}_6^{\alpha-\beta} + e_2\bar{z}_1^{\beta-1}z_2^{\alpha-\beta}z_4^{\alpha-\beta}\bar{z}_5^\beta + \mathcal{O}(|\mathbf{z}|^{2\alpha}), \quad (4)$$

where  $\mathbf{u} \equiv (|z_1|^2, |z_2|^2, |z_3|^2, |z_4|^2, |z_5|^2, |z_6|^2)$ , and  $\mathbf{q} \equiv (z_1 z_2 z_3, z_4 z_5 z_6, \bar{z}_1 \bar{z}_2 \bar{z}_3, \bar{z}_4 \bar{z}_5 \bar{z}_6)$ , with

$$h_1(0, 0) = 1 + \lambda, \quad h_2(0, 0) \equiv \epsilon.$$

The discrete hexagonal symmetries place some further restrictions on the functions  $h_1, h_2$  and also determine the other components of  $\mathbf{f}$  from  $f_1$ ; see [6] for details. Dionne, *et al.* [6] showed that the ‘resonant terms’ with coefficients  $e_1, e_2$  are important in calculating the stability properties of patterns that involve all six critical Fourier modes  $z_1, \dots, z_6$ ; they do not affect the stability of small-amplitude stripes, rhombs, and hexagons, which involve 1, 2, and 3 critical Fourier modes, respectively.

We now focus on patterns that have at least three-fold rotational symmetry. These can be investigated by restricting the bifurcation problem (3) to the subspace

$$\mathbf{z}(m) = (u_m, u_m, u_m, v_m, v_m, v_m), \quad (5)$$

where  $u_m$  and  $v_m$  are complex Fourier amplitudes measured at time  $t = mT$ . In order to simplify our presentation we set  $\alpha = 3, \beta = 2$  in (4). The results for general  $\alpha, \beta$  are qualitatively the same.

We first recall some results about period-one simple hexagons which satisfy  $(u_m, v_m) = (Re^{i\varphi}, 0)$  or  $(0, Re^{i\varphi})$ , where the amplitude  $R$  and phase  $\varphi$  obey

$$\begin{aligned} 0 &= \lambda + \epsilon R \cos(3\varphi) + AR^2 + \dots \\ 0 &= \sin(3\varphi) \left( -\epsilon + BR^2 + \dots \right). \end{aligned} \quad (6)$$

Here  $A$  and  $B$  are nonlinear coefficients that arise from the Taylor expansions of  $h_1$  and  $h_2$  in (4). The solutions of (6) that bifurcate from the origin at  $\lambda = 0$  satisfy  $\sin(3\varphi) = 0$ ; the hexagons with  $\varphi = 0, \pm\frac{2\pi}{3}$  are related by translations, as are the hexagons with  $\varphi = \pi, \pm\frac{\pi}{3}$ . These two sets of hexagons, ‘up-hexagons’ (denoted  $H^+$ ) and ‘down-hexagons’ (denoted  $H^-$ ), lie on the two branches associated with a transcritical bifurcation. In non-Boussinesq convection, these states correspond to ones in which fluid is rising or falling in the center of the hexagonal convection cells [5].

We now consider patterns that involve all six complex Fourier modes  $z_1, \dots, z_6$  in (3). Specifically, we investigate period-one solutions with  $u_m = v_m = \rho e^{i\psi}$  in (5). We find that the amplitude  $\rho$  and the phase  $\psi$  satisfy equations of the form, *cf.* (6),

$$\begin{aligned} 0 &= \lambda + \epsilon \rho \cos(3\psi) + \tilde{A}\rho^2 + \dots \\ 0 &= \sin(3\psi) \left( -\epsilon + \tilde{B}\rho^2 + \dots \right) + E\rho^3 \sin(2\psi) + \dots \end{aligned} \quad (7)$$

for  $\alpha = 3$ ,  $\beta = 2$  and  $(e_1 - e_2) \equiv E$  in (4). We see that in this case there are two distinct types of solutions that bifurcate from the origin at  $\lambda = 0$ ; those with phase  $\psi = 0, \pi$  and those with  $\psi \approx \pm\pi/3, \pm 2\pi/3$ . Unlike the case of simple hexagons, these solutions are not related by a translation of the patterns. The solutions with  $\psi = 0, \pi$  have hexagonal symmetry; in [6] they are referred to as ‘super hexagons’. Such hexagonal states were recently observed as nonlinear optical patterns [10]. As in the case of the simple hexagons, the super hexagons appear in a transcritical bifurcation with the two branches satisfying  $\psi = 0$  and  $\psi = \pi$ , respectively. The solutions satisfying  $\psi \approx \pm\pi/3, \pm 2\pi/3$  have only triangular symmetry, and are new. The triangular solutions with  $\psi \approx 2\pi/3$  and  $\psi \approx -\pi/3$  are the two branches of a transcritical bifurcation; a rotation of these patterns by  $\pi$  changes the sign of  $\psi$ . These solutions have an identical structure to the superlattice-I harmonic state described in [1]: compare Figure 1 with Figure 3 which shows an example of the triangular harmonic wave pattern. All of the solutions just described bifurcate *simultaneously* from the origin at  $\lambda = 0$ . Moreover, we know that the solutions with  $\cos(3\varphi) > 0$  in (6) and  $\cos(3\psi) > 0$  in (7) bifurcate in the same direction from the origin, as do the branches with  $\cos(3\varphi), \cos(3\psi) < 0$ , *e.g.*, if  $\epsilon < 0$  then the branches with  $\cos(3\varphi), \cos(3\psi) < 0$  bifurcate subcritically, while those satisfying  $\cos(3\varphi), \cos(3\psi) > 0$  are supercritical.

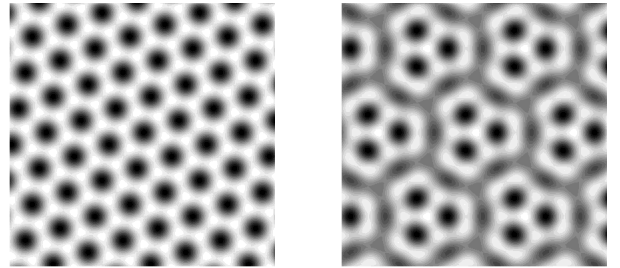


FIG. 3. Examples of patterns, periodic on a hexagonal lattice, that bifurcate transcritically from the flat state. These are plots of the appropriate superpositions of the critical Fourier modes associated with the wave vectors  $\pm\mathbf{K}_1, \dots, \pm\mathbf{K}_6$  in Figure 2. The plots are, left to right, down-hexagons ( $H^-$ ) and large down-triangles ( $T^-$ ) (*cf.* Figure 1). The critical wavenumber  $k_c$  dictates the size of the small scale structure evident in the superlattice pattern.

All of the known primary solution branches are unstable at bifurcation due to the presence of the quadratic nonlinear term in (4). In order to obtain stable small-amplitude solutions we need to assume that  $|\epsilon| \ll 1$ , where  $\epsilon$  is the coefficient of the quadratic term in the bifurcation problem. If the high-order resonant terms, with coefficients  $e_1, e_2$  in (4), are neglected then the large hexagonal and triangular solutions satisfying (7) are at best neutrally stable because an extra Floquet multiplier  $\mu$  (of multiplicity two) satisfies  $\mu = 1$ . While there is a unit multiplier of multiplicity two associated with translations of the pattern, the extra multiplier results from a symmetry of the truncated equations that allows a relative translation of the two rotated hexagons that make up the pattern. This symmetry of the equations is broken by the resonant terms and the Floquet multiplier then moves off the unit circle. For  $\alpha = 3$ ,  $\beta = 2$  in (4),  $\mu > 1$  for the super hexagons if  $4e_1 + 5e_2 < 0$  [6]. Analogously, we can show that  $\mu < 1$  for the large triangles if  $4e_1 + 5e_2 < 0$ . Thus if the large hexagons and triangles are neutrally stable when the high-order resonant terms are neglected, then one and only one of them is in fact stable (at least for sufficiently small amplitudes). It should be noted that the multiplier needed to determine relative stability of the large patterns cannot be computed within the subspace (5).

In Figure 4, we present part of a bifurcation diagram associated with the stroboscopic map (3) for the particular example

$$\begin{aligned} f_1 &= (1 + \lambda)z_1 + \epsilon\bar{z}_2\bar{z}_3 - (2|z_1|^2 + |z_2|^2 + |z_3|^2)z_1 \\ &\quad - (0.5|z_4|^2 + 0.6|z_5|^2 + 0.7|z_6|^2)z_1 + z_1z_4z_5z_6 \\ &\quad + 2(|z_2|^2 + |z_3|^2)\bar{z}_2\bar{z}_3 - z_3^2z_4^2\bar{z}_6 - 2\bar{z}_1z_2z_4\bar{z}_5^2, \end{aligned} \quad (8)$$

where  $0 < |\epsilon| \ll 1$ . This example demonstrates that it is possible to reproduce the type of transition observed by Kudrolli, Pier and Gollub [1] within the framework of a generic bifurcation problem on a hexagonal lattice.

Specifically, it shows a hysteretic transition between the flat state and small hexagons, followed by another hysteretic transition between the hexagons and the large triangular pattern as the bifurcation parameter is increased. The other primary branches (stripes, rhombs and super hexagons) are all unstable in this case and are not shown. Note that for  $\epsilon < 0$  the transition is between the down-states depicted in Figure 3, while if  $\epsilon > 0$  the transition is between up-states.

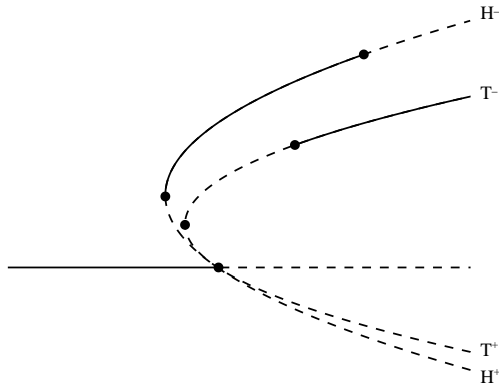


FIG. 4. Part of the bifurcation diagram associated with the bifurcation problem (8) for  $-1 \ll \epsilon < 0$ . Bifurcation points are indicated by solid circles. Only branches of small hexagons ( $H^\pm$ ) and large triangles ( $T^\pm$ ) are indicated; solid lines correspond to stable solutions. Other *unstable* branches, such as stripes, rhombs and super hexagons, that bifurcate simultaneously with these solutions, are not shown. Branches produced in secondary bifurcations are also not shown.

While the foregoing analysis shows compellingly that it is *possible* to achieve the transitions observed in the experiments, for completeness of the theory it would of course be necessary to calculate the nonlinear coefficients in (4) from the hydrodynamic equations and check that certain inequalities, required for stability, are obeyed. This is a non-trivial task since, as we have shown, certain details of the stability calculations depend on high-order resonant interaction terms. Moreover, the analysis is only strictly valid for  $|\epsilon| \ll 1$ . Zhang and Viñals have used a quasi-potential approximation to the Navier-Stokes equation, valid for very low viscosity fluids, to compute cubic coefficients in the case that subharmonic waves are preferred [11]. It would clearly be of interest to extend their quantitative results in a systematic exploration of parameter space to explore the range of possibilities uncovered by our qualitative analysis.

In our calculations, which make use of a stroboscopic map and thus assume a ‘snapshot’ of the surface, there is a clear distinction between the up- and down-states. In the subharmonic case these states are related by a time-translation symmetry, and Kudrolli and Gollub [12] have indeed observed the instantaneous co-existence of

up- and down-hexagons in that situation. On the other hand, in the case of two-frequency forcing of harmonic waves, there is a distinction between up and down even at the level of the linear eigenfunction which generically has a mean part. We thus expect this distinction between up- and down-hexagons to arise not only in the snapshots but also within time averages. This is in contrast to the subharmonic case with sinusoidal forcing where any time-average signal is presumably due to nonlinear effects resulting either from finite amplitude disturbances or else from properties of the experimental imaging optics.

Finally, we note that all our calculations have assumed that the solutions are strictly periodic on a hexagonal lattice. For the present parameters this is certainly an excellent model of the observations. But as noted in [1] for different values of the parameters the realized solution is a quasi-pattern. It is not clear what feature of the present problem leads to the spatially *periodic* superlattice state. A mechanism for favoring quasi-patterns by a resonant interaction between two bifurcating states with different horizontal wavenumbers was proposed by Edwards and Fauve [3]. Whether a similar resonance mechanism is responsible for the spatially-periodic superlattice patterns is an intriguing, open question which will be the subject of a future investigation.

We thank J.P. Gollub and A. Kudrolli for discussing their experiments with us. We also thank H. Riecke and A.C. Skeldon for helpful discussions. This research was supported by a NATO collaborative research grant CRG-950227. The research of MS is supported by NSF grant DMS-9404266, and by an NSF CAREER award DMS-9502266. The research of MREP is supported by the UK PPARC and EPSRC.

---

- [1] A. Kudrolli, B. Pier and J.P. Gollub, preprint (1997).
- [2] J.W. Miles and D. Henderson, Annu. Rev. Fluid Mech. **22**, 143 (1990).
- [3] W.S. Edwards and S. Fauve, J. Fluid Mech. **278**, 123 (1994).
- [4] T. Besson, W. Stuart Edwards and L.S. Tuckerman, Phys. Rev. E **54**, 507 (1995).
- [5] F.H. Busse, Rep. Prog. Phys. **41** 1929 (1978).
- [6] B. Dionne, M. Silber and A.C. Skeldon, Nonlinearity **10**, 321 (1997).
- [7] M.C. Cross and P.C. Hohenberg, Rev. Mod. Phys. **65**, 851 (1993).
- [8] M.R.E. Proctor and P.C. Matthews, Physica D **97**, 229 (1996).
- [9] B. Dionne and M. Golubitsky, ZAMP **43**, 36 (1992).
- [10] E. Pampaloni, S. Residori, S. Soria, and F.T. Arecchi, Phys. Rev. Lett. **78**, 1042 (1997).
- [11] W. Zhang and J. Viñals, preprint (1997).
- [12] A. Kudrolli and J.P. Gollub, Physica D **97**, 133 (1996).